Dalton Transactions

ROYAL SOCIETY OF CHEMISTRY

COMMUNICATION

View Article Online
View Journal | View Issue

Cite this: *Dalton Trans.*, 2025, **54**, 8400

Received 23rd April 2025,
Accepted 6th May 2025

DOI: 10.1039/d5dt00946d

rsc.li/dalton

A comparative study on *nido*- and *closo*-carborane supported zinc-salen catalysts for the ROCOP of epoxides and anhydrides†

Jin-Bian Xue,‡ Jia-Ni Wang,‡ Ke-Cheng Chen, Qian Cheng, Jia-Ying Zhang and Xu-Qiong Xiao *

***Nido*- and *closo*-carborane supported Zn–salen complexes (2–4) were prepared. The *nido*-C_2B_9 carborane anion supported Zn–salen complexes are superior to the *closo*-carborane supported ones in ROCOP of epoxides and anhydrides. These findings show the importance of electronic effects in the backbone of the salen ligands and offer guidance for future catalyst design.**

Polyesters represent a class of polymers that are not only versatile but also hold potential for sustainability and biodegradability.[1] These materials find extensive applications across various fields, ranging from packaging to biomedical devices. One particularly promising approach for synthesizing polyesters is the ring-opening copolymerization (ROCOP) of epoxides and cyclic anhydrides.[2] This method offers significant advantages, including the ability to finely tune the properties of the resulting polyesters by modifying the structures of the epoxide and cyclic anhydride monomers. Furthermore, ROCOP proceeds under relatively mild reaction conditions.[3] The continued advancement of this polymerization technique is largely driven by innovations in catalyst design, which play a crucial role in enhancing its efficiency and expanding its applicability.[4] Although numerous catalytic systems have been developed, metallic catalysts based on salen ligands remain highly attractive due to their ease of accessibility, tunable electronic and steric properties, and ability to coordinate with a wide range of metals in various oxidation states. These features enable the design of versatile catalysts with alterable Lewis acidic metal centers and optimized coordination environments. Among these metal–salen catalysts, Zn-based complexes stand out for their low cost, low toxicity, controlled reactivity and selectivity and their abundance on Earth.[5]

On the other hand, 1,2-dicarba-*closo*-dodecaboranes (*o*-carboranes) and their derivatives have received considerable attention since their first synthesis in 1963, owing to their unique cage-like structures and applications in medicine, nonlinear optical materials, luminescent materials, and coordination/organometallic chemistry.[6] Among these, *closo*- and *nido*-carboranes are the most extensively studied due to their distinct structural and electronic properties.[7] For example, the *o*-carborane cluster as a whole can exhibit electron-withdrawing properties when attached to other systems like organometallic complexes or substituted derivatives, while *nido*-carboranes are stronger electron donors as they carry a negative charge.[8] These remarkable differences are particularly important in coordination or organometallic complexes when they are employed as auxiliary ligands. In this contribution, we report the preparation of *nido*-C_2B_9 carborane anion- and *o*-carborane-supported zinc–salen complexes and a comparative study of their catalytic abilities in ROCOP of epoxides and anhydrides.

The *o*-carborane-supported salen ligands (**1a–1d**) were synthesized according to literature procedures.[9] Complexation with zinc was initially carried out using the common zinc salt, $Zn(OAc)_2$. Treatment of ligands **1a–1d** with $Zn(OAc)_2$ in ethanol at room temperature for 24 hours afforded the corresponding complexes **2a–2d**. (Scheme 1) The absence of pheno-

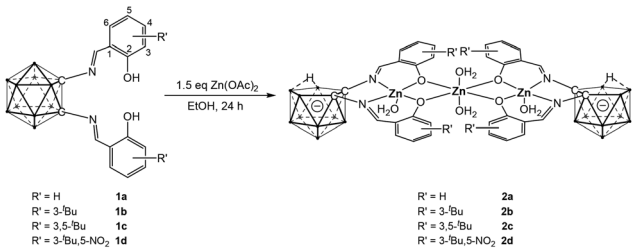

Scheme 1 Synthesis of trinuclear zinc complexes **2a–2d**.

Key Laboratory of Organosilicon Chemistry and Material Technology, Ministry of Education, Zhejiang Key Laboratory of Organosilicon Material Technology, College of Material, Chemistry and Chemical Engineering, Hangzhou Normal University, No. 2318 Yuhangtang Rd. Hangzhou, 311121 Zhejiang, China.
E-mail: xqxiao@hznu.edu.cn

†Electronic supplementary information (ESI) available: Experimental details, NMR spectra, X-ray crystallographic data. CCDC 2444573–2444575. For ESI and crystallographic data in CIF or other electronic format see DOI: https://doi.org/10.1039/d5dt00946d

‡These authors contributed equally.

lic proton signals in the ^{1}H NMR spectra confirmed successful complexation, while the ^{11}B NMR spectra exhibited resonances between −10 ppm and −39 ppm, indicative of *o*-carborane cage opening.[10] The formation of the zinc complexes was further corroborated by single-crystal X-ray diffraction (SCXRD) analysis (Fig. 1).

The molecular structure of complex **2a** is shown in Fig. 1 (see also Fig. S59,† with selected bond lengths and angles in the caption). The solid-state structure clearly reveals that the salen-Zn units are supported by *nido*-C_2B_9 carborane anions, consistent with the ^{11}B NMR data. Remarkably, two of these *nido*-carborane-supported salen–Zn moieties are bridged by a third Zn(II) ion, forming a trinuclear complex. The two *nido*-carborane units adopt a face-to-face arrangement, with their [ONNO] coordination planes nearly parallel. Together with the third Zn(II) ion, these two C_2B_3 and two [ONNO] planes form a channel-like structure. Unlike previously reported multinuclear Zn(II) complexes, which often feature a dangling methoxy group as an additional donor ligand,[11] no such group is present here. The Zn(1) center adopts a pentacoordinate environment with a τ_5 value of 0.04,[12] suggesting a near-ideal square pyramidal geometry, whereas Zn(2) displays a hexacoordinate geometry. The Zn(1)–Zn(2) distance is 312.77(7) pm, shorter than the sum of their van der Waals radii (410 pm), suggesting a weak metal–metal interaction.

To obtain both *nido*-C_2B_9 carborane anion- and *o*-carborane-supported salen complexes, complexation reactions were subsequently carried out using $ZnCl_2$. Treatment of ligands **1a–1d** with anhydrous $ZnCl_2$ in the presence of Et_3N under reflux in THF yielded yellow complexes. (Scheme 2) The ^{11}B NMR spectra displayed resonances in the range of −9.56 to −35.08 ppm, and the ^{1}H NMR spectrum exhibited a broad

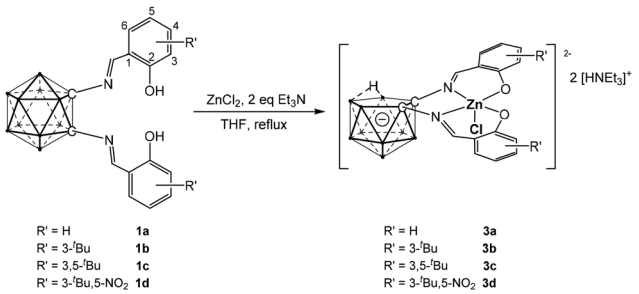

Scheme 2 Synthesis of zinc complexes **3a–3d**.

signal at −2.3 ppm, both indicative of cage opening of the *closo*-carborane. The molecular structure of the anionic part of complex **3b** is shown in Fig. 2 (see also Fig. S60†). It is clearly shown that the Zn(1) center was supported by the *nido*-C_2B_9 carborane anion and adopted a pentacoordinate geometry, with a chloride ligand occupying the apical position in addition to the four donor atoms of the salen ligand. The calculated τ_5 value is 0.33, indicating a distorted square pyramidal geometry. The asymmetric unit of **3b** clearly contains two [$HNEt_3$] moieties.

A structural comparison between complexes **2a** and **3b** suggests that Zn(2) in **2a** plays a similar role to the triethylammonium cation in **3b**, serving to balance the negative charge of the *nido*-C_2B_9 carborane moieties. The conversion of **2** to **3** was achieved by treatment with excess [$HNEt_3$]Cl in CH_2Cl_2. It is documented that elevated temperatures induced cage opening. Consequently, reactions of **1** with $ZnCl_2$ in the presence of 2 equivalents of Et_3N were performed at room temperature (Scheme 3). The ^{11}B NMR spectrum showed peaks

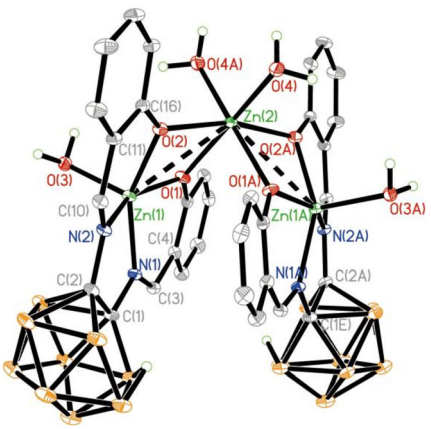

Fig. 1 Molecular structure of complex **2a** (some of the hydrogen atoms are omitted for clarity; ellipsoids are set at the 30% probability level). Selected bond lengths (Å) and angles (°): C(1)–C(2) 1.594(6), Zn(1)–Zn(2) 3.1277(7), Zn(1)–O(1) 1.993(3), Zn(1)–O(2) 1.981(3), Zn(1)–N(1) 2.042(3), Zn(1)–N(2) 2.044(3), Zn(2)–O(1) 2.103(3), and Zn(2)–O(2) 2.123(3); O(1)–Zn(1)–O(3) 97.09(12), O(1)–Zn(1)–N(1) 89.98(12), O(1)–Zn(1)–N(2) 152.95 (13), O(2)–Zn(1)–O(1) 81.70(11), O(2)–Zn(1)–O(3) 100.86(12), O(2)–Zn(1)–N(1) 150.72(13), O(2)–Zn(1)–N(2) 91.72(12), N(1)–Zn(1)–O(3) 108.03(13), N(1)–Zn(1)–N(2) 83.02(13) and N(2)–Zn(1)–O(3) 109.93(13).

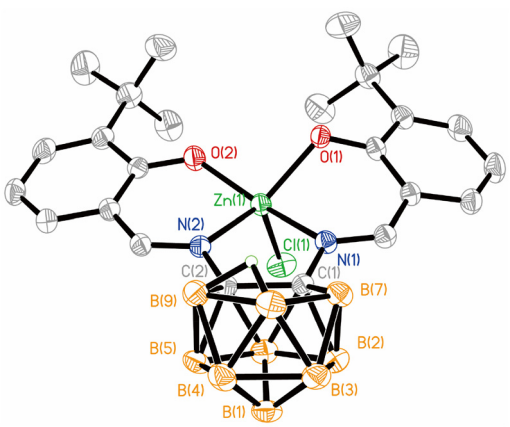

Fig. 2 Molecular structure of complex **3b** (some of the hydrogen atoms are omitted for clarity; ellipsoids are set at the 30% probability level). Selected bond lengths (Å) and angles(°): C(1)–C(2) 1.584(4), Zn(1)–Cl(1) 2.3454(13), Zn(1)–O(1) 2.027(2), Zn(1)–O(2) 1.955(2), Zn(1)–N(1) 2.133(3), and Zn(1)–N(2) 2.107(2); O(1)–Zn(1)–Cl(1) 107.51(7), O(1)–Zn (1)–N(1) 82.54(9), O(1)–Zn(1)–N(2) 137.85(9), O(2)–Zn(1)–Cl(1) 103.43(8), O(2)–Zn(1)–O(1) 95.10(8), O(2)–Zn(1)–N(1) 157.74(10), O(2)–Zn(1)–N(2) 88.52(9), N(1)–Zn(1)–Cl(1) 98.35(8), N(2)–Zn(1)–Cl(1) 112.41(7), and N(2)–Zn(1)–N(1) 78.91(10).

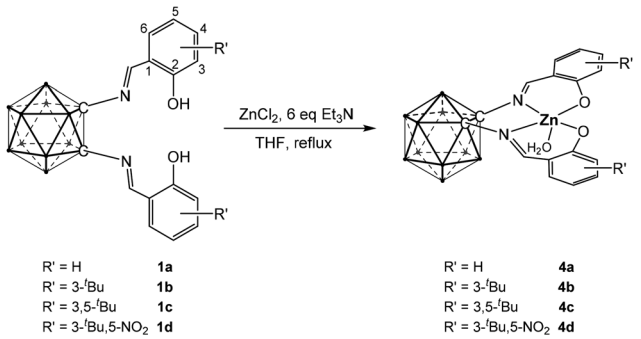

Scheme 3 Synthesis of zinc complexes **4a–4d**.

between −7.22 ppm and −15.68 ppm, indicating that deboronation did not occur, while ^{1}H NMR showed persistent phenolic proton signals with reduced integration, suggesting incomplete deprotonation. To address this, the reaction was repeated using excess Et_3N (*ca.* 6 equivalents), successfully affording complexes **4** (Scheme 3). Alternatively, deprotonation of **1** with *n*-BuLi followed by $ZnCl_2$ addition also afforded complexes **4**. However, the method outlined in Scheme 3 avoids the use of *n*-BuLi, providing a milder synthetic route.

Single crystals suitable for XRD analysis for **4a** were obtained by slow diffusion of hexane into a dichloromethane solution. The molecular structure of **4a** is depicted in Fig. 3 (see also Fig. S61†). It clearly demonstrates that the salen ligand is supported by a *closo*-carborane framework. The Zn centers adopt an ideal square pyramidal geometry, as indicated by a τ_5 value of 0.00. The C1–C1A bond length is 166.7(5) pm, whereas the corresponding distances in complexes **2a** and **3b** are 159.4(6) and 158.4(4) pm, respectively. For comparison, the typical C–C bond distance in *o*-carborane is approximately 162 pm.[13] These values clearly indicate that the *nido*- and *closo*-carborane ligands exert different electronic effects on the salen framework, which may, in turn, influence the catalytic activity of the corresponding complexes.

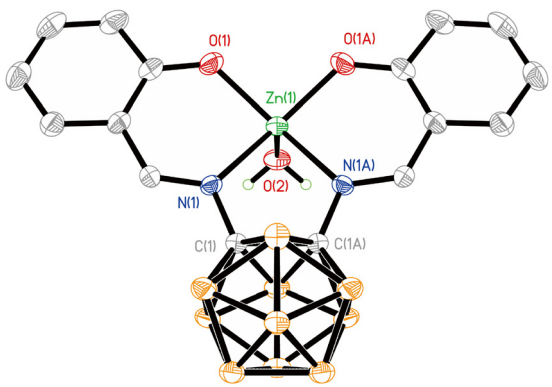

Fig. 3 Molecular structure of complex **4a** (some of the hydrogen atoms are omitted for clarity; ellipsoids are set at the 30% probability level). Selected bond lengths (Å) and angles(°): C1–C(1A) 1.667(5), Zn1–O1 1.973(2), Zn1–O2 2.012(3), Zn1–N1 2.124(2), N1–C1 1.421(3), and N1–C2 1.291(3); O(1A)–Zn1–O1 92.87(13), O(1A)–Zn1–O2 102.20(9), O1–Zn1–O2 102.20(9), O1–Zn1–N1 87.59(9), O1–Zn1–N(1A) 153.88(10), O(1A)–Zn1–N1 153.88(10), O(1A)–Zn1–N(1A) 87.59(9), O2–Zn1–N(1A) 103.21(9), O2–Zn1–N1 103.21(9), and N(1A)–Zn1–N1 80.87(12).

With complexes **2–4** in hand, their catalytic activities in the ROCOP of phthalic anhydride (PA) and cyclohexene oxide (CHO) were evaluated and compared (Table 1). Initial reactions were carried out using a molar ratio of 1 : 2 : 100 : 100 for the Zn catalyst, co-catalyst (bis(triphenylphosphine)iminium chloride, PPNCl), PA, and CHO, respectively, at an elevated temperature of 80 °C. As shown in entries 1–3 (Table 1), all complexes **2a–4a** exhibited activity for the ROCOP, affording polyesters with conversions ranging from 46% to 71%. A possible mechanism is proposed in Scheme 3. It involves activation of the epoxide by the metal center, followed by nucleophilic attack by a halide or carboxylate. This generated an alkoxide intermediate, which subsequently reacts with an anhydride to form a new ester linkage, incorporating one complete repeat unit and regenerating both a carboxylate and an open coordination site on the metal centre (Scheme 4).

The catalytic activity decreased in the order **3a** > **2a** > **4a**. Notably, the *nido*-carborane-supported mononuclear complex **3a** exhibited the highest activity under these conditions. These results suggest that *nido*-carborane-supported salen ligands outperform their *closo*-carborane counterparts due to differing electronic effects. The *nido*-carborane acts as an electron-donating group due to its negative charge, whereas *closo*-carborane is electron-withdrawing, as electron density can delocalize over its 3D cage structure. Comparing the two *nido*-carborane-based complexes **2a** and **3a**, it appears that the molecular structure plays a critical role. As discussed above, the structure of **2a** forms a "channel" through the coordination of two salen–Zn moieties with a third bridging Zn center. This

Table 1 The ROCOP of PA and CHO catalyzed by complexes **2–4** [a]

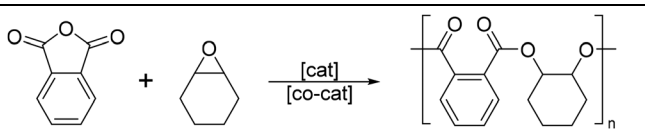

Entry	Cat.	Co-cat.[b]	T (°C)	t (h)	Yield[c]	M_n[d] (kDa)	PDI[d]
1	**2a**	2	80	16	46%	1.4	1.13
2	**3a**	2	80	16	71%	3.4	1.76
3	**4a**	2	80	16	40%	1.4	1.13
4	**3b**	2	80	16	85%	1.7	1.24
5	**3c**	2	80	16	74%	1.4	1.17
6	**3d**	2	80	16	67%	1.1	1.16
7	**3b**	1	80	16	40%	1.8	1.47
8	**3b**	4	80	16	90%	2.4	1.05
9	**3b**	4	80	1	18%	1.3	1.01
10	**3b**	4	80	8	63%	1.3	1.29
11	**3b**	4	80	24	87%	1.3	1.38
12	**3b**	4	50	16	14%	1.7	1.16
13	**3b**	4	110	16	98%	1.9	1.37

[a] Polymerization was performed in 5 mL of toluene with PPNCl as the cocatalyst. [b] Molar ratio to the catalyst. [c] Yield = weight of polymer obtained/weight of monomer used. [d] M_n and PDI were determined by GPC analysis calibrated with standard polystyrene samples.

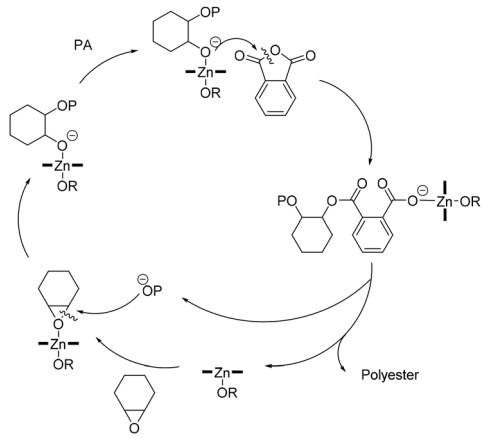

Scheme 4 Proposed mechanism for ROCOP.

Table 2 The substrate scope of epoxides catalysed by complex **3b**[a]

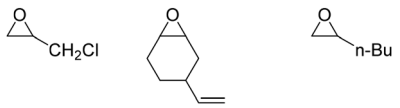

I II III

Entry	Substrates	Yield[b]	M_n[c] (kDa)	PDI[c]
1	**I**	50%	2.6	1.87
2	**II**	87%	2.3	1.29
3	**III**	72%	2.9	1.29

[a] Polymerization was performed in 5 mL of toluene. Molar ratio of catalyst to co-catalyst: 1 : 4. Temperature: 110 °C; reaction time: 16 hours. [b] Yield = weight of polymer obtained/weight of monomer used. [c] M_n and PDI were determined by GPC analysis calibrated with standard polystyrene samples.

channel likely limits substrate accessibility, thereby reducing catalytic efficiency.

The catalytic performance of complexes **3a–3d** was further investigated. Substituents on the phenyl ring also influenced the ROCOP activity, with complex **3b** outperforming **3a**, **3c**, and **3d** (entries 2 and 4–6). In our previous work, Al-based complexes with unsubstituted phenyl rings showed superior activity in the cycloaddition of epoxides and CO_2 at atmospheric pressure. We propose that the enhanced performance of **3b** may be attributed to an optimal balance of steric and electronic effects.

The effect of the catalyst-to-cocatalyst ratio was also examined. As shown in entries 4, 7, and 8, increasing the ratio from 1 : 1 to 1 : 4 led to a progressive improvement in yield. Thus, a 1 : 4 catalyst/cocatalyst ratio was adopted as optimal. It is important to note that the cocatalyst alone was inactive under similar conditions. Extending the reaction time improved yields (entries 4 and 9–11); however, beyond 16 hours, the increase was marginal (85% *vs.* 87%), establishing 16 hours as the optimal reaction time. Lowering the temperature to 50 °C significantly reduced the conversion to 14% (entry 12), while increasing the temperature to 110 °C improved the conversion to 98% (entry 13), making 110 °C the preferred temperature. This enhancement is likely due to increased solubility and mobility of both the polymer and phthalic anhydride at higher temperatures. Based on these findings, the optimal reaction conditions were established as a 1 : 4 catalyst/cocatalyst ratio, a reaction time of 16 hours, and a temperature of 110 °C. Notably, all resulting polyesters exhibited narrow molecular weight distributions, with polydispersity indices (PDIs) ranging from 1.01 to 1.76. Following optimization of the model PA/CHO ROCOP, various co-monomers were explored to assess the scope for producing structurally diverse polyesters. As summarized in Table 2, catalyst **3b** demonstrated good to high activity in the ROCOP of epichlorohydrin, 4-vinylcyclohexene oxide, and 1,2-epoxyhexane with PA.

In summary, a series of zinc complexes supported by *nido*- and *closo*-carborane-functionalized salen ligands were successfully synthesized. Structural analyses revealed that the *closo*-carborane-supported complexes are mononuclear, while the *nido*-carborane-supported complexes can adopt either mononuclear or trinuclear architectures. In all cases, the [ONNO]-coordinated zinc centers are pentacoordinate, with an oxygen-containing solvent molecule occupying the axial position. These complexes exhibited high catalytic activity in the ROCOP of epoxides with PA at elevated temperatures, affording polyesters with narrow polydispersity indices. Under comparable conditions, the *nido*-carborane-supported zinc complexes demonstrated superior catalytic performance compared to their *closo*-carborane counterparts, which is attributed to the electron-donating character of the negatively charged *nido*-C_2B_9 carborane ligand. These findings provide valuable insights into the structure–activity relationship in carborane-based catalysts for ROCOP and may offer a foundation for the rational design of advanced catalysts. Comparative studies on *nido*- and *closo*-carborane-supported ligands in other systems and their catalytic abilities are currently ongoing in our laboratory.

Data availability

The experimental details, NMR spectra, and X-ray crystallographic details that support the findings of this work have been uploaded as part of the ESI.†

CCDC 2444573–2444575 for **2a**, **3b** and **4a** contain the supplementary crystallographic data for this paper.†

Conflicts of interest

There are no conflicts to declare.

Acknowledgements

We gratefully acknowledge financial support from the National Natural Science Foundation of China (Grant No. 22471050 and

22171063) and the Natural Science Foundation of Zhejiang Province (Grant No. LY22B010002).

References

1 (*a*) C. Shi, E. C. Quinn, W. T. Diment and E. Y. X. Chen, *Chem. Rev.*, 2024, **124**, 4393–4478; (*b*) C. V. Aarsen, A. Liguori, R. Mattsson, M. H. Sipponen and M. Hakkarainen, *Chem. Rev.*, 2024, **124**, 8473–8515.

2 Z. B. Xie, Z. J. Yang, C. Y. Hu, F. Q. Bai, N. N. Li, Z. W. Wang, S. T. Ku, X. Pang, X. S. Chen and X. H. Wang, *J. Am. Chem. Soc.*, 2025, **147**, 12115–12126.

3 (*a*) F. Vidal, S. Smith and C. K. Williams, *J. Am. Chem. Soc.*, 2023, **145**, 13888–13900; (*b*) G. L. Gregory and C. K. Williams, *Macromolecules*, 2022, **55**, 2290–2299.

4 (*a*) J. R. Lamb, A. K. Hubbell, S. N. MacMillan and G. W. Coates, *J. Am. Chem. Soc.*, 2020, **142**, 8029–8035; (*b*) J. M. Longo, M. J. Sanford and G. W. Coates, *Chem. Rev.*, 2016, **116**, 15167–15197; (*c*) H.-Y. Ji, B. Wang, L. Pan and Y.-S. Li, *Green Chem.*, 2018, **20**, 641–648; (*d*) R. Xie, Y. Wang, S. Li, B. Li, J. Xu, J. Liu, Y. He, G. W. Yang and G. P. Wu, *Angew. Chem., Int. Ed.*, 2024, e202404207; (*e*) Y. Y. Zhang, G. W. Yang, R. Xie, L. Yang, B. Li and G. P. Wu, *Angew. Chem., Int. Ed.*, 2020, **59**, 23291–23298; (*f*) S. Li, S. Y. Liu, R. Yan, R. Xie, Q. Q. Xue, B. Li and G. P. Wu, *Chem. – Eur. J.*, 2025, **31**, e202500571.

5 (*a*) M. Winkler, C. Romain, M. A. R. Meier and C. K. Williams, *Green Chem.*, 2015, **17**, 300–306; (*b*) P. K. Saini, C. Romain, Y. Zhu and C. K. Williams, *Polym. Chem.*, 2014, **5**, 6068–6075.

6 (*a*) T. L. Heying, J. W. Ager, S. L. Clark, D. J. Mangold, H. L. Goldstein, M. Hillman, R. J. Polak and J. W. Szymanski, *Inorg. Chem.*, 1963, **2**, 1089–1092; (*b*) R. N. Grimes, *Carboranes*, Elsevier, Amsterdam, 3rd edn, 2016; (*c*) R. N. Grimes, *Chem. Rev.*, 1992, **92**, 251–268; (*d*) S. Liu, Y. F. Han and G. X. Jin, *Chem. Soc. Rev.*, 2007, **36**, 1543–1560; (*e*) Z. Qiu and Z. Xie, *Chem. Soc. Rev.*, 2022, **51**, 3164–3180; (*f*) Z. Z. Qiu and Z. W. Xie, *Acc. Chem. Res.*, 2021, **54**, 4065–4079; (*g*) R. Cheng, J. Zhang, H. Zhang, Z. Qiu and Z. Xie, *Nat. Commun.*, 2021, **12**, 7146; (*h*) I. Guerrero, Z. Kelemen, C. Viñas, I. Romero and F. Teixidor, *Chem. – Eur. J.*, 2020, **26**, 5027–5036.

7 (*a*) H. Y. Ren, N. N. Zhou, W. L. Ma, P. Zhang, D. S. Tu, C. S. Lu and H. Yan, *J. Am. Chem. Soc.*, 2024, **146**, 26543–26555; (*b*) H. T. Zhang, Y. Gao, Y. N. Ma and X. N. Chen, *Org. Chem. Front.*, 2024, **11**, 6706–6711; (*c*) F. Chen, W. Guo, Y.-N. Ma and X. Chen, *Chem. Commun.*, 2024, **60**, 614–617; (*d*) Y. N. Ma, H. Z. Ren, Y. X. Wu, N. Li, F. J. Chen and X. N. Chen, *J. Am. Chem. Soc.*, 2023, **145**, 7331–7342; (*e*) P. Farras, E. J. Juarez-Perez, M. Lepsik, R. Luque, R. Nuñez and F. Teixidor, *Chem. Soc. Rev.*, 2012, **41**, 3445–3463; (*f*) H. B. Yang, Y. Guo, K. Cao, Q. J. Jiang, C. C. Teng, D. Y. Zhu and S. H. Wang, *Chem. Commun.*, 2024, **60**, 1124–1127; (*g*) K. Cao and C. Y. Zhang, *Eur. J. Org. Chem.*, 2022, e202200737; (*h*) J. Jiao, P. He, T. L. Yang, T. W. Zhang, L. H. Wang, T. Han, Y. Nie, Z. Y. Lin and P. F. Li, *Org. Chem. Front.*, 2023, **10**, 5965–5970; (*i*) J. X. Li, L. J. Zhou, Y. P. Zhang, Y. X. Luo, M. Wu, P. F. Cui and G. X. Jin, *Eur. J. Inorg. Chem.*, 2025, **28**, e202400752; (*j*) D. K. Semyonov, G. K. Slushko, M. Y. Stogniy, S. A. Anufriev, I. A. Godovikov, K. Y. Suponitsky, V. I. Bregadze and I. B. Sivaev, *Organometallics*, 2023, **42**, 2522–2530.

8 (*a*) A. M. Spokoyny, *Pure Appl. Chem.*, 2013, **85**, 903–919; (*b*) Z. Z. Cui, B. N. Wang, J. X. Li, R. L. Pang, Y. R. Kang and X. Q. Xiao, *Chin. J. Chem.*, 2021, **39**, 2410–2416.

9 (*a*) Y. R. Kang, B. N. Wang, R. X. Nan, Y. W. Li, Z. L. Zhu and X. Q. Xiao, *Inorg. Chem.*, 2022, **61**, 8806–8814; (*b*) B. N. Wang, Z. L. Zhu, M. J. Liang, Y. K. Ren, J. B. Xue, J. Y. Zhang, F. Qi and X. Q. Xiao, *Inorg. Chem.*, 2024, **63**, 5481–5486; (*c*) R. X. Nan, Y. W. Li, Z. L. Zhu, F. Qi and X. Q. Xiao, *J. Am. Chem. Soc.*, 2023, **145**, 15538–15546; (*d*) Y. K. Ren, Y. Li, M. J. Liang, J. W. Ma, Z. X. Niu and X. Q. Xiao, *Inorg. Chem.*, 2025, **64**, DOI: **10.1021/acs.inorgchem.5c00935**.

10 (*a*) T. Y. He and R. A. Musah, *Polyhedron*, 2019, **163**, 171–177; (*b*) L. J. Todd and A. R. Siedle, *Prog. Nucl. Magn. Reson. Spectrosc.*, 1979, **13**, 87–176.

11 (*a*) A. Thevenon, J. A. Garden, A. J. P. White and C. K. Williams, *Inorg. Chem.*, 2015, **54**, 11906–11915; (*b*) M. Ghosh, S. Biswas, M. Roy, S. Biswas, P. Ghosh, S. Koner, S. Mandal and S. Saha, *New J. Chem.*, 2021, **45**, 12296–12304.

12 (*a*) N. Ikpo, S. M. Barbon, M. W. Drover, L. N. Dawe and F. M. Kerton, *Organometallics*, 2012, **31**, 8145–8158; (*b*) A. W. Addison, T. N. Rao, J. Reedijk, J. van Rijn and G. C. Verschoor, *J. Chem. Soc., Dalton Trans.*, 1984, 1349–1356.

13 (*a*) R. Pang, J. Li, Z. Cui, C. Zheng, Z. Li, W. Chen, F. Qi, L. Su and X. Q. Xiao, *Dalton Trans.*, 2019, **48**, 7242–7248; (*b*) J. Li, R. Pang, Z. Li, G. Lai, X. Q. Xiao and T. Müller, *Angew. Chem., Int. Ed.*, 2019, **58**, 1397–1401; (*c*) D. Buzsáki, D. Gál, B. Szathmári, T. Holczbauer, A. Udvardy, J. K. Szilágyiné, D. Kargin, C. Bruhn, R. Pietschnig and Z. Kelemen, *Inorg. Chem. Front.*, 2025, **12**, 1822–1830.

